ACS Sustainable Chemistry & Engineering

Research Article

pubs.acs.org/journal/ascecg

Eggshell Membrane-Supported Recyclable Catalytic Noble Metal Nanoparticles for Organic Reactions

Ramakrishna Mallampati and Suresh Valiyaveettil*

Department of Chemistry, National University of Singapore, 3 Science Drive 3, Singapore 117543

Supporting Information

ABSTRACT: Heterogeneous catalysts are used in many industrial processes. Here, we report a simple method for a template-assisted synthesis of nanoparticle catalysts and for testing their catalytic efficiency toward two model organic reactions. Eggshell membrane (ESM) reduced metal cations to metal atoms, stabilized the nanoparticles, and was used as a supporting material for the nanoparticles. The gold and silver nanoparticles were characterized using UV−vis spectroscopy, FESEM, XRD, and XPS studies. As a proof of concept, the resultant membrane-supported nanoparticles were used as a heterogeneous catalyst for the reduction of p-nitrophenol and synthesis of propargylamine. High recyclability of the reactions indicates that nanoparticles are strongly attached to the eggshell membrane surface. Easy synthesis, high catalytic activity, and recyclability make these catalysts interesting for further studies.

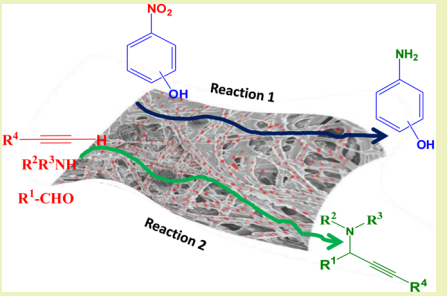

KEYWORDS: *A^3 coupling, Catalyst, Eggshell membrane, Reduction, Template*

INTRODUCTION

Functional nanoparticles are used in different areas of material science such as catalysis,[1] electrochemistry,[2] bioimaging,[3] and sensing.[4−6] Gold and silver nanoparticles (NPs) are particularly interesting due to their ease of preparation and control over size and shape using conventional synthesis.[7−10] Synthetic methods for preparing various nanoparticles have been reviewed recently.[11−18] The use of biotemplates such as chitosan, plant extracts, and protein fibrils for the synthesis of nanoparticles was explored recently.[19−23] Nanostructured noble metals such as Au, Ag, and Pt have been used as catalysts for a variety of organic reactions owing to high surface to volume ratios and high surface energy that enhances catalytic activity.[24,25] Heterogeneous catalysis offers easy separation, recycling of the catalyst, and product purification. The catalytic metal NPs are usually supported on a substrate such as metal oxide,[26] active carbon,[27] or stabilized by polymer molecules.[28] Porous supports offer ordered pores with controllable size, high surface area, and large pore volume,[29] which can be used for the stabilization of metal NPs catalysts.[30] Catalysts supported on porous substrates face problems such as difficulty in characterization, possibly clogging the pores, and not being accessible to reagents. Therefore, it is important to look for an alternative support with excellent textural characteristics and surface properties for the fabrication of highly stable catalytic NPs.

Herein, we report the synthesis of monodispersed Au and Ag NPs with a size range of 10−25 nm on the surface of eggshell membrane (ESM) support. Use of natural waste material such as ESM with abundant functional groups such as $-NH_2$, $-OH$, and $-CHO$[31] on the surface helps to reduce, reuse, and recycle waste materials. The functional groups on the fiber surfaces of ESM act as stabilizing and reducing agents, which removes the need for additional reagents, surface modification, or capping agents for the nanoparticles. The fibrous nature of the ESM offers a large surface area for immobilization of catalysts particles. It is also interesting to test the NPs on ESM surfaces for their stability, catalytic activity, and recyclability in various organic reactions. Catalytic performance of the NPs was evaluated using two different model reactions such as reduction of nitrophenols and one-pot synthesis of functionalized propargylamines.

EXPERIMENTAL SECTION

Materials and Synthesis. Fresh eggs from the local supermarket were gently broken. The contents were removed, and the shells were washed with water. The white semipermeable eggshell membrane was carefully peeled and cleaned with deionized water. The clean ESM (100 mg) was dried in air at ambient conditions, cut into small pieces (4 mm^2), and immersed in aqueous solutions of $HAuCl_4$ and AgNO3 (10 mL, 5 mM). The solutions were stirred at room temperature (30 °C) for 2 h. The metal salt solutions slowly decolorized, and the white ESM was turned to a light red color for the gold solution and a gray color for the silver solution. No additional reducing agents were added. Ag cations require relatively longer time (48 h) for reduction on the ESM surface. The NP-immobilized ESMs (NP-ESMs) were removed from the solutions after 12 h and rinsed with copious amounts of deionized water to remove excess nonreduced metal salts. The samples were placed in clean glass Petri dishes and left for 24 h at room temperature (30 °C) in dark for drying. The dry samples were stored in a glass bottle without further processing. The density of the NPs on the membrane can be controlled by varying the noble metal solution concentration. NPs were prepared using several concentrations of

Received: November 25, 2013
Revised: January 9, 2014
Published: January 13, 2014

metal ions, and the nanofibers incorporated with nanoparticles at the lowest concentration (5 mM) were used for all reactions to reduce the amount of metal (Figure S1, Supporting Information) without causing significant reduction in catalytic conversions.

Characterization of the Samples. X-ray diffraction (XRD) patterns of the samples were recorded using a Bruker-AXS D8 DISCOVER with GADDS powder X-ray diffractometer with Cu Kα (λ = 1.54 Å) at 40 kV and 40 mA over a range of 2θ angle from 2° to 80°. The morphology of the ESM and NPs were examined using a JEOL JSM-6701F field emission scanning electron micrograph (FESEM). Energy dispersive X-ray spectroscopy (EDS) was used for identification and quantification of elements in the material. UV−vis spectra of NP-ESMs were recorded on a Shimadzu UV-1601 PC spectrophotometer. Surface elements of the peels were identified using X-ray photoelectron spectroscopy (XPS) with a spatial resolution of 30 μm (Kratos XPS system, Axis His, 165 Ultra, Shimadzu, Japan). The XPS results were collected in binding energy form and fit using a nonlinear least-squares curve fitting program (XPSPEAK41 software). The peak's full width at half-maximum (fwhm) was fixed during the fitting.

RESULTS AND DISCUSSION

Owing to the presence of large amounts of functional groups (−OH, $-CO_2H$, $-NH_2$, −CHO), it is conceivable that the surface-adsorbed Au (III) or Ag (I) cations get reduced to nanoparticles on the ESM. This can be verified using SEM, XPS, and visible changes in color of the ESM. SEM images of the natural ESM and NPs adsorbed on to the surface are given in Figure 1. It has been reported that collagen and saccharides

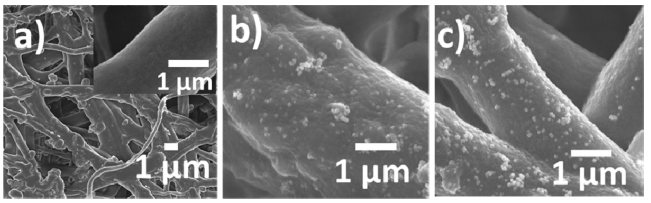

Figure 1. SEM images of natural ESM (a), Au NPs (b), and Ag NPs (c) on ESM fibers.

are the main constituents of ESM fibers. Nakano et al.[31] reported that the main chemical constituents of chicken ESM are amino acids (glycine and alanine) and uronic acid. The aldehyde moiety of uronic acid and saccharides in ESM play a significant role in reducing the surface-adsorbed metal ions to NPs.[32] In addition, other groups such as $-NH_2$ and −OH also interact with Au (III) or Ag (I) ions. The presence of NPs on the surface of ESM was also established using energy dispersive spectroscopy (EDS) (Figure S2, Supporting Information). Samples were coated with Pt by using a sputtering process before SEM and EDS analysis for enhancing the conductivity. A spot profile energy dispersive X-ray analysis of the NPs showed characteristic Au (0) peaks at 2.12 and 9.78 keV and a Ag (0) peak at 3.1 keV. Oxidation states of gold and silver species in NPs were studied using XPS (Figure 2), which showed characteristic Au (4f) and Ag (3d) peaks in the spectrum. Binding energies of 370 eV for the Ag $3d_{5/2}$ peak and 87.7 eV for the Au $4f_{7/2}$ peaks were also observed. The XPS results are in good agreement with SEM and EDS data that zero valent gold and silver atoms were formed on the surface of ESM. UV−vis spectra were recorded for NP-ESMs (Figure 3a) to study the size and optical properties of nanoparticles. Small pieces of ESM composites were used to record UV−vis spectra in reflectance mode with BaSO4 as reference material. Broad

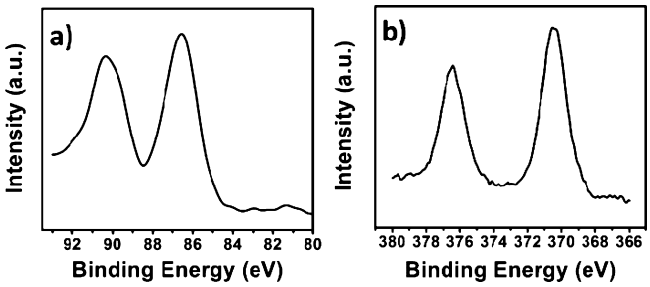

Figure 2. XPs spectra of Au NP (a) and Ag NP (b) on ESM. Spectra were recorded using ESM-NPs.

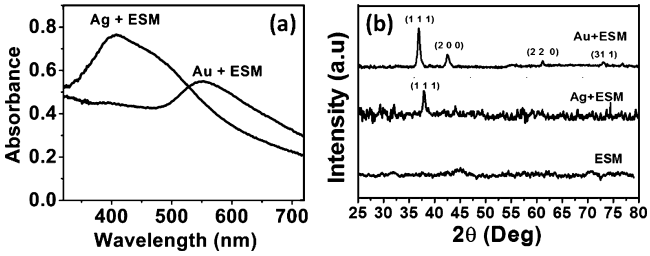

Figure 3. UV−vis spectra (a) and XRD pattern (b) of Au-ESM and Ag-ESM at ambient conditions.

surface plasmon resonance (SPR) absorption peaks with maximum at 514 nm for Au and 400 nm for Ag were observed. These results are consistent with previous reports on the synthesis of NPs. X-ray diffraction studies were performed to confirm the presence of NPs on ESM fibers and to study the crystalline nature of those NPs. The XRD patterns of ESM and NP-ESMs are shown in Figure 3b. All peaks were indexed and compared with reported literature values. Significant peaks corresponding to Au (111), (200), (220), (311), and (222) lattice planes confirm the presence of Au (JCPDS 7440-57-5) and peaks corresponding to Ag (111) lattice plane confirm the presence of Ag (JCPDS 7440-22-4) on ESM.

Reduction of p-Nitrophenol. Aromatic amines are widely used in the synthesis of pharmaceuticals, dyes, and agrochemicals.[33,34] Two general methods were used for the reduction of aromatic nitrocompounds in industry, which include stoichiometric reduction[35] and catalytic hydrogenation.[36,37] The catalytic hydrogenation is a convenient method for producing amines in high yield. Reduction of aromatic nitrocompounds using various nanoparticles prepared by different techniques has been investigated earlier[38−40] and suffers from limitations in reusability and recovery of the catalyst after the reaction. Biotemplated nanoparticles as catalysts have been explored owing to the fact that they can be recovered easily and reused a number of times.[41] Here, we investigated the efficiency of NP-ESMs as catalysts for the borohydride reduction of p-nitrophenol, owing to the solubility of nitrophenols in water. In the absence of Au-ESM, the mixture of p-nitrophenol and $NaBH_4$ showed an absorption maximum at 400 nm corresponding to the p-nitrophenolate ion. This peak was unchanged with time indicating that the reduction did not take place; however, the addition of a small amount of NP-ESMs to the above reaction mixture caused fading of the yellow color of the reaction mixture in quick succession. Time-dependent absorption spectra of this reaction mixture showed the disappearance of the peak at 400 nm and a gradual development of a new peak at 300 nm corresponding to the formation of p-aminophenol (Figure 4). Similarly,

dx.doi.org/10.1021/sc4004899 | ACS Sustainable Chem. Eng. 2014, 2, 855−859

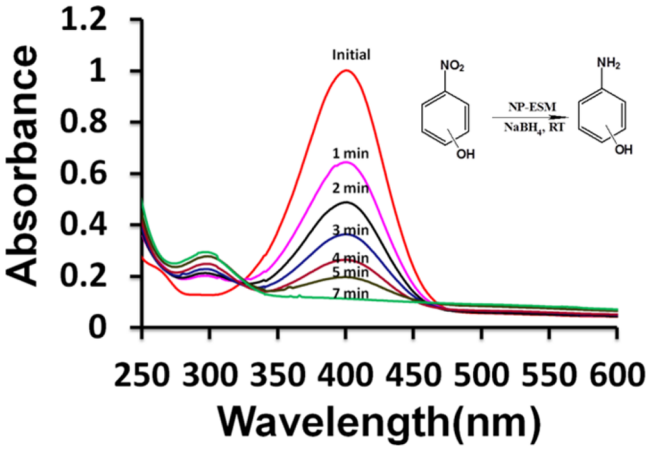

Figure 4. Time-dependent UV–vis spectra of the reduction of p-nitrophenol by Au-ESM with time.

borohydride reduction of o- and m-nitrophenol in the presence of NP-ESMs were also investigated under similar conditions (Figure S3, Supporting Information). The changes in the spectral patterns are similar to that observed in the case of p-nitrophenol reduction. These results indicated that NP-ESMs can successfully catalyze the reduction of o-nitrophenol and m-nitrophenol. Apparent rate constants (k_{app}) were calculated for all reactions from the graph of ln A vs time (Figure S4, Supporting Information), where A is absorbance. For comparison, the catalytic data of all three reactions are presented in Table 1. The data shows that the rate of p-nitrophenol reduction catalyzed by NP-ESMs is higher than that of other two nitrophenols and follows the order of p-nitrophenol > o-nitrophenol > m-nitrophenol. Such differences in the reaction rate might be due to the influence of position of substituents. Generally, the rate of reduction of nitrophenols depends on the formation and stability of nitrophenolate ions that can be explained in more detail by comparing the resonance structure of three isomeric nitrophenolate ions.[42] In the case of the o- and p-nitrophenolate ion, the $-NO_2$ group is in resonance with the negative charge on oxygen that is delocalized throughout the benzene ring and hence stabilized. However, due to steric hindrance, the influence of the $-I$ (inductive) effect of the $-NO_2$ group in the o-nitrophenolate ion is relatively less than in the p-nitrophenolate ion. In the case of m-nitrophenol, the $-NO_2$ group cannot enter into direct resonance stabilization of the negative charge on oxygen and exert only a weak negative inductive effect. Therefore, the rate of reduction of different isomeric nitrophenols follows the order of p-nitrophenol > o-nitrophenol > m-nitrophenol. Ag-NPs showed higher activity as compared to Au-NPs.

Table 1. k_{app} of Different Borohydide Reduction Reactions in the Presence of Au + ESM and Ag + ESM

	apparent rate constant ($k_{app/S}^{-1}$)		
catalyst	2-aminophenol	4-aminophenol	3-aminophenol
Au-ESM	3.2×10^{-3}	6.3×10^{-3}	1.6×10^{-3}
Ag-ESM	5.6×10^{-3}	11.2×10^{-3}	2.5×10^{-3}

Reusability of the catalyst due to easy separation is another advantage of heterogeneous catalysts over homogeneous catalysts in industrial applications. Although, many catalytic studies have been reported in the literature using nanoparticles as catalysts, there are only a few reports where the catalysts were recovered for further use in consecutive cycles. In order to check the reusability, ESM-NPs were recovered and reused in repeated reduction reactions of p-nitrophenol. Generally, catalytic activity decreases with the number of reaction cycles, and the reaction times for complete conversion among the consecutive runs are recorded (Table S1, Supporting Information). These results indicate that the NP-ESMs are active up to five cycles of nitrophenol reduction. After each reaction, the reaction mixture was analyzed for the presence of Au and Ag using ICP-OES. There was no detectable amount of Au and Ag in the reaction mixture, which indicates no significant loss of nanoparticles from ESM during the reaction. This also highlights the high stability and recyclability of the catalyst without significant decrease in activity.

Synthesis of Propargylamine. One-pot multicomponent coupling reactions (MCR), where several organic moieties are coupled in one step, is an attractive synthetic strategy.[43,44] The three-component coupling of aldehydes, amines, and alkynes (A^3 coupling) is an example of MCR and has received much attention in recent times.[45] The propargylamine derivatives obtained from A^3 coupling reactions are useful as synthetic intermediates for the synthesis of biologically active compounds such as β-lactams, conformationally restricted peptides, natural products, and therapeutic drug molecules.[46−48] Traditionally, propargylamines are prepared by the amination of propargylic halides, propargylic phosphates, or propargylic triflates.[49,50] However, these reagents used in stoichiometric amounts are highly moisture sensitive and require controlled reaction conditions. Development of improved synthetic methods for the synthesis of propargylamines remained as an active area of research.[51] Recently, metal NPs, especially Au and Ag NPs with high surface to volume ratio have been used to activate the C–H bond of the terminal alkynes.[52] However, metal NPs in their pure form tend to agglomerate, which limits their efficiency in the catalytic processes. Herein, highly dispersed Au and Ag NPs grown over ESM were used as catalysts for the synthesis of propargylamines by an A^3 coupling reaction. This reaction shows the catalytic activity of NP-ESMs even in organic solvent. The catalytic efficiency of NP-ESMs was tested in three-component coupling of aldehyde, amine, and alkyne. Initially, benzaldehyde (1 mmol), piperidine (1.2 mmol), and phenylacetylene (1.2 mmol) were mixed with NP-ESMs (20 mg) in toluene (20 mL). The reaction was carried out at 100 °C and completed in 24 h with a quantitative yield of the final product (Figure 5). Formation of the product was confirmed by spectroscopic methods. These results prompted us to study the

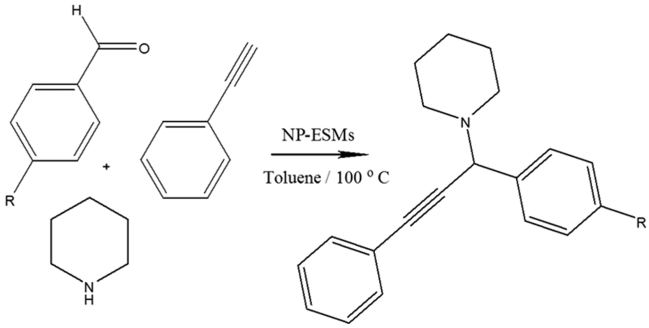

Figure 5. Nanoparticles catalyzed coupling reactions to form propargylamine derivatives.

dx.doi.org/10.1021/sc4004899 | ACS Sustainable Chem. Eng. 2014, 2, 855–859

substituent effects on the aromatic ring of benzaldehydes. For example, p-methylbenzaldehyde furnished the desired product in good yield (99%), whereas no reaction was observed when p-nitrobenzaldehyde was used (Table S2, Supporting Information). No product was formed in the absence of catalyst or in the presence of pure ESM under identical conditions. It is understood that the A^3 coupling reaction proceeds by terminal alkyne C−H bond activation by NPs on ESM.[50] The NP acetylide intermediate then reacts with the iminium ion formed in situ from the aldehyde and the amine to generate the corresponding propargylamine. The reusability of the catalysts was demonstrated for five consecutive reactions. The membrane-supported catalyst was recovered by filtration through filter paper (pore size: 12 μm) followed by washing with toluene. The recovered catalyst was used for consecutive reactions. Results (Table S3, Supporting Information) indicate that the NP-ESMs showed significant catalytic activity up to five cycles of reaction. The morphology and stability of the catalyst after the fifth cycle of the reaction was observed through SEM (Figure 6), which clearly shows the presence of NPs on ESM

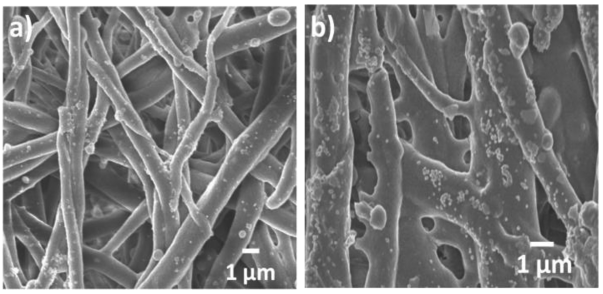

Figure 6. FESEM images of Au-ESM (a) and Ag-ESM (b) after five consecutive reactions.

indicating that the NPs were stable on ESM and did not leach out during the reaction. Many groups have reported transition metal-based compounds as catalysts for A^3 coupling reactions.[44,48,52] However, tedious synthesis, poor recovery, and high toxicity of these catalysts make them not suitable for many applications. High abundance, low cost, low toxicity, biodegradability, and easy handling of the ESM-supported nanocatalysts described here are versatile and can be used to perform a series of reactions both in aqueous and organic media.

CONCLUSIONS

Readily available ESM was employed for the synthesis of metal NPs using the surface functionalities for the autoreduction of metal ions. Immobilizing NPs on ESM enabled easy handling of the catalyst compared to free nanoparticles. Catalytic efficiencies of NP-ESMs were evaluated for two different types of reactions. NP-ESM catalysts can be used for the efficient reduction of nitro groups to amines within a short period of time (10 min) in water and A^3 coupling reactions with high yield (99%) in organic medium. It is believed that these simple catalytic systems can be further explored for other important organic reactions. Our catalysts offer an added advantage in terms of low cost, nontoxicity, easy synthesis, and reusability. The ESM template is verstile, green, and cost-effective to offer many fascinating possibilities for designing new catalysts for different reactions in both organic and aqueous phases and is expected to be useful in industrial applications.

ASSOCIATED CONTENT

Supporting Information

More characterization data (EDS analysis) of ESM-NPs and different reaction yields. This material is available free of charge via the Internet at http://pubs.acs.org.

AUTHOR INFORMATION

Corresponding Author

*Tel.: (65) 65164327. Fax: (65) 67791691. E-mail: chmsv@nus.edu.sg.

Notes

The authors declare no competing financial interest.

ACKNOWLEDGMENTS

The authors acknowledge the financial support of the National University of Singapore through research grants and support from the technical staff at the Department of Chemistry. R.M. acknowledges a graduate scholarship from the National University of Singapore.

REFERENCES

(1) Narayanan, R.; El-Sayed, M. A. Catalysis with transition metal nanoparticles in colloidal solution: Nanoparticle shape dependence and stability. *J. Phys. Chem. B* **2005**, *109*, 12663−12676.
(2) Rashid, M. H.; Bhattacharjee, R. R.; Kotal, A.; Mandal, T. K. Synthesis of spongy gold nanocrystals with pronounced catalytic activities. *Langmuir* **2006**, *22*, 7141−7143.
(3) Rashid, M. H.; Mandal, T. K. Synthesis and catalytic application of nanostructured silver dendrites. *J. Phys. Chem. C* **2007**, *111*, 16750−16760.
(4) Rashid, M. H.; Bhattacharjee, R. R.; Mandal, T. K. Organic ligand-mediated synthesis of shape-tunable gold nanoparticles: An application of their thin film as refractive index sensors. *J. Phys. Chem. C* **2007**, *111*, 9684−9693.
(5) Li, C.-Z.; Male, K. B.; Hrapovic, S.; Luong, J. H. T. Fluorescence properties of gold nanorods and their application for DNA biosensing. *Chem. Commun.* **2005**, *0*, 3924−3926.
(6) Xia, Y.; Yang, P.; Sun, Y.; Wu, Y.; Mayers, B.; Gates, B.; Yin, Y.; Kim, F.; Yan, H. One-dimensional nanostructures: Synthesis, characterization, and applications. *Adv. Mater.* **2003**, *15*, 353−389.
(7) Sun, Y.; Xia, Y. Shape-controlled synthesis of gold and silver nanoparticles. *Science* **2002**, *298*, 2176−2179.
(8) Hao, E.; Bailey, R. C.; Schatz, G. C.; Hupp, J. T.; Li, S. Synthesis and optical properties of "branched" gold nanocrystals. *Nano Lett.* **2004**, *4*, 327−330.
(9) Suzuki, M.; Niidome, Y.; Kuwahara, Y.; Terasaki, N.; Inoue, K.; Yamada, S. Surface-enhanced nonresonance raman scattering from size- and morphology-controlled gold nanoparticle films. *J. Phys. Chem. B* **2004**, *108*, 11660−11665.
(10) Murphy, C. J.; Sau, T. K.; Gole, A. M.; Orendorff, C. J.; Gao, J.; Gou, L.; Hunyadi, S. E.; Li, T. Anisotropic metal nanoparticles: Synthesis, assembly, and optical applications. *J. Phys. Chem. B* **2005**, *109*, 13857−13870.
(11) Kim, F.; Song, J. H.; Yang, P. Photochemical synthesis of gold nanorods. *J. Am. Chem. Soc.* **2002**, *124*, 14316−14317.
(12) Gole, A.; Murphy, C. J. Seed-mediated synthesis of gold nanorods: Role of the size and nature of the seed. *Chem. Mater.* **2004**, *16*, 3633−3640.
(13) Jin, R.; Egusa, S.; Scherer, N. F. Thermally-induced formation of atomic Au clusters and conversion into nanocubes. *J. Am. Chem. Soc.* **2004**, *126*, 9900−9901.

(14) Seo, D.; Park, J. C.; Song, H. Polyhedral gold nanocrystals with Oh symmetry: From octahedra to cubes. *J. Am. Chem. Soc.* **2006**, *128*, 14863−14870.
(15) Li, C.; Shuford, K. L.; Park, Q. H.; Cai, W.; Li, Y.; Lee, E. J.; Cho, S. O. High-yield synthesis of single-crystalline gold nano-octahedra. *Angew. Chem., Int. Ed.* **2007**, *46*, 3264−3268.
(16) Kwon, K.; Lee, K. Y.; Lee, Y. W.; Kim, M.; Heo, J.; Ahn, S. J.; Han, S. W. Controlled synthesis of icosahedral gold nanoparticles and their surface-enhanced raman scattering property. *J. Phys. Chem. C* **2006**, *111*, 1161−1165.
(17) Chen, H. M.; Hsin, C. F.; Liu, R.-S.; Lee, J.-F.; Jang, L.-Y. Synthesis and characterization of multi-pod-shaped gold/silver nanostructures. *J. Phys. Chem. C* **2007**, *111*, 5909−5914.
(18) Chu, H.-C.; Kuo, C.-H.; Huang, M. H. Thermal aqueous solution approach for the synthesis of triangular and hexagonal gold nanoplates with three different size ranges. *Inorg. Chem.* **2005**, *45*, 808−813.
(19) Colby, R.; Hulleman, J.; Padalkar, S.; Rochet, J. C.; Stanciu, L. A. Biotemplated synthesis of metallic nanoparticle chains on an alpha-synuclein fiber scaffold. *J. Nanosci. Nanotechnol.* **2008**, *8*, 973−8.
(20) Hall, S. R.; Collins, A. M.; Wood, N. J.; Ogasawara, W.; Morad, M.; Miedziak, P. J.; Sankar, M.; Knight, D. W.; Hutchings, G. J. Biotemplated synthesis of catalytic Au−Pd nanoparticles. *RSC Advances* **2012**, *2*, 2217−2220.
(21) Iwahori, K.; Yamashita, I. Bio-template synthesis of nanoparticle by cage-shaped protein supramolecule, apoferritin. *J. Cluster Sci.* **2007**, *18*, 358−370.
(22) Behrens, S.; Unger, E.; Wu, J.; Habicht, W.; Dinjus, E. Biotemplate synthesis of Ag nanoparticles and nanowires. *MRS Online Proc. Libr.* **2004**, *818*, null−null.
(23) Vijayaraghavan, K.; Nalini, S. P. K. Biotemplates in the green synthesis of silver nanoparticles. *Biotechnol. J.* **2010**, *5*, 1098−1110.
(24) Miyamura, H.; Matsubara, R.; Miyazaki, Y.; Kobayashi, S. Aerobic oxidation of alcohols at room temperature and atmospheric conditions catalyzed by reusable gold nanoclusters stabilized by the benzene rings of polystyrene derivatives. *Angew. Chem., Int. Ed.* **2007**, *46*, 4151−4154.
(25) Kanaoka, S.; Yagi, N.; Fukuyama, Y.; Aoshima, S.; Tsunoyama, H.; Tsukuda, T.; Sakurai, H. Thermosensitive gold nanoclusters stabilized by well-defined vinyl ether star polymers: Reusable and durable catalysts for aerobic alcohol oxidation. *J. Am. Chem. Soc.* **2007**, *129*, 12060−12061.
(26) Enache, D.; Knight, D.; Hutchings, G. Solvent-free oxidation of primary alcohols to aldehydes using supported gold catalysts. *Catal. Lett.* **2005**, *103*, 43−52.
(27) Carrettin, S.; McMorn, P.; Johnston, P.; Griffin, K.; Hutchings, G. J. Selective oxidation of glycerol to glyceric acid using a gold catalyst in aqueous sodium hydroxide. *Chem. Commun.* **2002**, *0*, 696−697.
(28) Praharaj, S.; Nath, S.; Ghosh, S. K.; Kundu, S.; Pal, T. Immobilization and recovery of Au nanoparticles from anion exchange resin: Resin-bound nanoparticle matrix as a catalyst for the reduction of 4-nitrophenol. *Langmuir* **2004**, *20*, 9889−9892.
(29) Fukuoka, A.; Higuchi, T.; Ohtake, T.; Oshio, T.; Kimura, J.-i.; Sakamoto, Y.; Shimomura, N.; Inagaki, S.; Ichikawa, M. Nanonecklaces of platinum and gold with high aspect ratios synthesized in mesoporous organosilica templates by wet hydrogen reduction. *Chem. Mater.* **2005**, *18*, 337−343.
(30) Besson, E.; Mehdi, A.; Reye, C.; Corriu, R. J. P. Soft route for monodisperse gold nanoparticles confined within SH-functionalized walls of mesoporous silica. *J. Mater. Chem.* **2009**, *19*, 4746−4752.
(31) Nakano, T.; Ikawa, N.; Ozimek, L. Chemical composition of chicken eggshell and shell membranes. *Poult. Sci.* **2003**, *82*, 510−514.
(32) Zheng, B.; Qian, L.; Yuan, H.; Xiao, D.; Yang, X.; Paau, M. C.; Choi, M. M. F. Preparation of gold nanoparticles on eggshell membrane and their biosensing application. *Talanta* **2010**, *82*, 177−183.
(33) Neilson, A.H. Anthropogenic Compounds, Part J: PAHs and Related Compounds: Biology. In *The Handbook of Environmental Chemistry*, Vol. *3*; Lewis Publishers: Boca Raton, FL, 1997, p 346.
(34) Schwab, C. E.; Huber, W. W.; Parzefall, W.; Hietsch, G.; Kassie, F.; Schulte-Hermann, R.; Knasmuller, S. Search for compounds that inhibit the genotoxic and carcinogenic effects of heterocyclic aromatic amines. *Crit. Rev. Toxicol.* **2000**, *30*, 1−69.
(35) Xu, S.; Xi, X.; Shi, J.; Cao, S. A homogeneous catalyst made of poly(4-vinylpyridine-co-N-vinylpyrrolidone)-Pd(0) complex for hydrogenation of aromatic nitro compounds. *J. Mol. Catal. A: Chem.* **2000**, *160*, 287−292.
(36) Downing, R. S.; Kunkeler, P. J.; van Bekkum, H. Catalytic syntheses of aromatic amines. *Catal. Today* **1997**, *37*, 121−136.
(37) Deshpande, R. M.; Mahajan, A. N.; Diwakar, M. M.; Ozarde, P. S.; Chaudhari, R. V. Chemoselective hydrogenation of substituted nitroaromatics using novel water-soluble iron complex catalysts. *J. Org. Chem.* **2004**, *69*, 4835−4838.
(38) Pradhan, N.; Pal, A.; Pal, T. Silver nanoparticle catalyzed reduction of aromatic nitro compounds. *Colloids Surf., A* **2002**, *196*, 247−257.
(39) Esumi, K.; Isono, R.; Yoshimura, T. Preparation of PAMAM− and PPI−Metal (silver, platinum, and palladium) nanocomposites and their catalytic activities for reduction of 4-nitrophenol. *Langmuir* **2003**, *20*, 237−243.
(40) Liu, J.; Qin, G.; Raveendran, P.; Ikushima, Y. Facile "green" synthesis, characterization, and catalytic function of β-D-glucose-stabilized Au nanocrystals. *Chem.—Eur. J.* **2006**, *12*, 2131−2138.
(41) Hayakawa, K.; Yoshimura, T.; Esumi, K. Preparation of gold−dendrimer nanocomposites by laser irradiation and their catalytic reduction of 4-nitrophenol. *Langmuir* **2003**, *19*, 5517−5521.
(42) Finar, I. L. *Organic Chemistry. The Fundamental Principles*, Vol. *1*, 6th ed.; English Language Book Society: London, U.K., 1973.
(43) Armstrong, R. W.; Combs, A. P.; Tempest, P. A.; Brown, S. D.; Keating, T. A. Multiple-component condensation strategies for combinatorial library synthesis. *Acc. Chem. Res.* **1996**, *29*, 123−131.
(44) Kamijo, S.; Yamamoto, Y. Synthesis of allyl cyanamides and N-cyanoindoles via the palladium-catalyzed three-component coupling reaction. *J. Am. Chem. Soc.* **2002**, *124*, 11940−11945.
(45) Ringdahl, B. *The Muscarinic Receptors*; Brown, J. H., Ed.; Humana Press: Clifton, N J, 1989, pp 377−418.
(46) Miura, M.; Enna, M.; Okuro, K.; Nomura, M. Copper-catalyzed reaction of terminal alkynes with nitrones. selective synthesis of 1-aza-1-buten-3-yne and 2-azetidinone derivatives. *J. Org. Chem.* **1995**, *60*, 4999−5004.
(47) Jenmalm, A.; Berts, W.; Li, Y.-L.; Luthman, K.; Csoeregh, I.; Hacksell, U. Stereoselective epoxidation of Phe−Gly and Phe−Phe vinyl isosteres. *J. Org. Chem.* **1994**, *59*, 1139−1148.
(48) Dyker, G. Transition metal catalyzed coupling reactions under C−H activation. *Angew. Chem., Int. Ed.* **1999**, *38*, 1698−1712.
(49) Imada, Y.; Yuasa, M.; Nakamura, I.; Murahashi, S.-I. Copper(I)-catalyzed amination of propargyl esters. Selective synthesis of propargylamines, 1-alken-3-ylamines, and (Z)-allylamines. *J. Org. Chem.* **1994**, *59*, 2282−2284.
(50) Czernecki, S.; Valéry, J.-M. A stereocontrolled synthesis of a lincosamine precursor. *J. Carbohydr. Chem.* **1990**, *9*, 767−770.
(51) Wei, C.; Li, C.-J. A highly efficient three-component coupling of aldehyde, alkyne, and amines via C−H activation catalyzed by gold in water. *J. Am. Chem. Soc.* **2003**, *125*, 9584−9585.
(52) Wei, C.; Li, Z.; Li, C.-J. The first silver-catalyzed three-component coupling of aldehyde, alkyne, and amine. *Org. Lett.* **2003**, *5*, 4473−4475.